analytical chemistry

Article

pubs.acs.org/ac

Second Harmonic Correlation Spectroscopy: A Method for Determining Surface Binding Kinetics and Thermodynamics

Krystal L. Sly, Sze-Wing Mok, and John C. Conboy*

Department of Chemistry, University of Utah, 315 South 1400 East RM. 2020, Salt Lake City, Utah 84112, United States

ABSTRACT: These studies describe the implementation of second harmonic correlation spectroscopy (SHCS) to measure the adsorption and desorption kinetics of molecular species associated with a surface. Specifically, the local fluctuations of the measured second harmonic (SH) signal were used to determine the binding kinetics and thermodynamics of (S)-(+)-1,1′-bi-2-napthol SBN intercalation into a 1,2-dioleoyl-*sn*-glycero-3-phosphocoline (DOPC) bilayer. In order to determine the adsorption and desorption rates, the SH signal was collected above saturation concentration at steady-state equilibrium as a function of time. The autocorrelated SH signal was then fit to a correlation model developed for molecules binding at a surface when there is no contribution from molecules in solution. The measured adsorption rate for SBN to DOPC was $2.7 \pm 0.2 \times 10^3$ s^{-1} M^{-1} and the desorption rate was $9 \pm 4 \times 10^{-4}$ s^{-1}. The kinetic rates as well as the calculated equilibrium binding constant, $3.0 \pm 1.3 \times 10^6$ M^{-1} obtained from SHCS were compared with those obtained from a conventional binding isotherm and found to be statistically consistent. The primary advantage of using SHCS is both the absorption and desorption rates were determined in the same experiment using only a single bulk concentration of SBN. The results of these studies demonstrate that SHCS can be used to provide accurate kinetic and thermodynamic binding data in a label-free manner in lieu of conventional isotherm studies, especially where time and analyte are scarce.

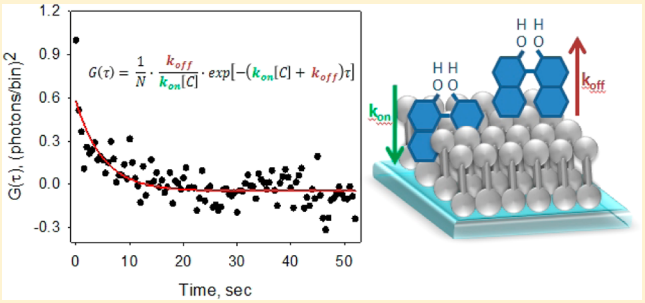

Fluorescence correlation spectroscopy (FCS) is a well-established statistical method where temporal fluctuations in the fluorescence signal from a sample of fluorescent molecules are used to characterize the molecular processes that give rise to these fluctuations.[1] FCS was utilized as early as the 1970s to determine the translational and rotational diffusion coefficients and kinetic rates of various species in bulk solution and on lipid bilayer membranes.[2−4] It has since been used to analyze lipid and protein diffusion,[5,6] protein aggregation,[7,8] and muscle contraction.[9] More recently FCS has been implemented to determine the surface binding kinetics of fluorescently labeled biomolecules.[10−16] For example, the reversible binding of fluorescently labeled IgG to albumin-coated surfaces and planar supported lipid bilayers (PSLB) doped with Fc receptors,[10,11] rhodamine 6G association to C18 functionalized surfaces,[12,13] and DNA hybridization at a water/glass interface have all be investigated using FCS.[16] In these studies, the temporal fluctuations in the fluorescence signal were measured from a small observation volume created using total internal reflection and autocorrelated to obtain information about the dynamics of interfacial binding. For molecules interacting with a surface, the measured temporal fluctuations arise from fluorescent molecules diffusing into and out of the evanescent excitation volume and from molecules associating to and dissociating from the surface or surface-bound receptor.[1,17] Although FCS theory has been extensively developed and implemented for such surface interactions,[12,17−19] the interpretation of the fluorescence autocorrelation data is complicated by fluorescence arising from species in solution, background fluorescence, and photobleaching. These contributions to the measured autocorrelation confound the analysis of the surface dynamic processes.[20] Small solution volumes and low analyte concentrations, down to the single-molecule detection level, have been used to circumvent these issues, but the barrier to a meaningful autocorrelation then becomes the time required to collect enough dynamic molecular events.[20]

Application of correlation spectroscopy to a label-free and surface specific technique such as second harmonic generation (SHG) would eliminate observable fluctuations from molecular diffusion in solution and ameliorate problems associated with the degradation of fluorophores without having to necessarily reduce the number of molecules in the observation area. For SHCS the only contributions to the measured temporal fluctuations in the signal will arise from surface associated species. This greatly simplifies data analysis and eliminates obstacles due to fluorescent molecules in bulk solution within the evanescent excitation volume. The added benefit of not needing a molecule to be fluorescent in order to be detected by SHG makes SHCS a label-free alternative to conventional FCS. As far as the authors know, correlation spectroscopy has not been applied to SHG to determine the binding kinetics of

Received: June 21, 2013
Accepted: August 8, 2013
Published: August 8, 2013

   dx.doi.org/10.1021/ac4018742 | *Anal. Chem.* 2013, 85, 8429−8435

molecules at a surface. In one instance, autocorrelation was used to extract the rotational diffusion coefficient of clay particles in solution for a SHG scattering experiment.[21] However, in this study by Yan and Eisenthal, the rotational diffusion dynamics giving rising to the measured fluctuations are vastly different from the dynamics at a surface as no molecular interaction contributed to the correlated data. In order to examine the molecular interactions at a surface, the new label-free and surface specific technique of SHCS described below is used to ascertain the binding kinetics and thermodynamics of a small molecule associating with a surface for the first time.

To demonstrate the feasibility of SHCS to effectively determine the binding kinetics of a molecule to a surface, the SHG active small molecule, (S)-(+)-1,1′-bi-2-napthol (SBN), associating with a 1,2-dioleoyl-*sn*-glycero-3-phosphocoline (DOPC) planar supported lipid bilayer (PSLB) is examined. The results obtained from SHCS are compared to a classical adsorption isotherm experiment to verify the accuracy of the kinetic and thermodynamic values retrieved from the SHCS analysis. Using SHCS, both the adsorption and desorption rates are simultaneously determined using only one steady-state concentration in a much shorter time period as compared to the conventional isotherm study. Thus, SHCS provides a more efficient and comprehensive method for studying molecular interactions at a surface without the need for an exogenous label.

SECOND HARMONIC CORRELATION SPECTROSCOPY THEORY

Autocorrelation is a method that can be easily applied to any system where measured population fluctuations can be cross-correlated with itself to extrapolate any correlated dynamic events on the time scale of the measured fluctuations. In a chemical system, the population fluctuations can arise from mass transport, diffusion (rotational and translational), or a chemical reaction.[13] In FCS, the fluctuations in the fluorescence signal are autocorrelated to reveal information regarding the dynamic molecular events occurring within the observation volume.[1] Similarly, in SHCS the measured fluctuations in SH signal can be measured as a function of time and correlated to determine dynamic molecular events.

The measured SH signal is proportional to the second-order susceptibility tensor, $\chi^{(2)}_{ijk}$ which is composed of a nonresonant $\chi^{(2)}_{NR}$ and resonant $\chi^{(2)}_{R}$ portion:

$$I_{SHG} \propto |\chi^{(2)}_{ijk}|^2 \propto |\chi^{(2)}_{NR} + \chi^{(2)}_{R}|^2 \quad (1)$$

The resonant $\chi^{(2)}_{R}$ contribution can be expressed as:[22]

$$(\chi^{(2)}_{ijk})_R \propto N \sum_{a,b,c} \frac{\langle a|\mu_i|c\rangle\langle a|\mu_j|b\rangle\langle b|\mu_k|c\rangle}{(2\hbar\omega - E_{ca} - i\Gamma_{ca})(\hbar\omega - E_{bc} - i\Gamma_{bc})} \quad (2)$$

where N is the surface density of molecules, h is Planck's constant, μ is the Cartesian coordinate dipole operator, Γ is the transition line width, and a, b, and c represent the initial, intermediate, and final states, respectively. The indices on $\chi^{(2)}_{ijk}$ denote the input (j,k) and output (i) fields which can assume any of the three Cartesian coordinates (x,y,z). As seen in the denominator of eq 2, the SH signal is enhanced when the incident, ω, or SH, 2ω, frequency is resonant with an electronic transition of a molecule at the interface; therefore, very low concentrations of an analyte can be detected.[23] In these studies a fundamental wavelength of 532 nm is used such that the resulting SH wavelength is 266 nm, which is in resonance with the electronic transition of the small molecule SBN (shown in Figure 1). The signal enhancement from this resonance allows detection down to nanomolar concentrations of SBN.[23,24]

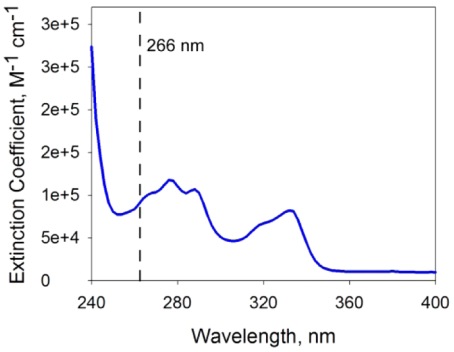

Figure 1. Extinction coefficient spectra of SBN.

Equations 1 and 2 also show that the SH signal is proportional to the surface density of molecules squared (N^2), which is unlike fluorescence where the measured signal is linearly proportional to N. A linear proportionality between the measured SH and the surface density of molecules can be achieved by subtracting the mean SH signal and taking the square-root, with the obvious caveat that positive and negative deviations must be treated separately (i.e., for negative deviations the quantity $-(|-\Delta SH|^{1/2})$ is used). As an approximation, when the mean of the SH signal is much larger than the fluctuations from the mean, as is normally the case, the fluctuations will appear to be linearly related to N, which simplifies the data analysis. Using either method, at equilibrium the fluctuations in the SH signal have a Gaussian distribution with the variance proportional to the size of the system.[24] The measured SH signal fluctuations about the mean as a function of time, t, can be described as[1]

$$\delta SH(t) = SH(t) - \langle SH\rangle \quad (3)$$

where $SH(t)$ is the measured fluctuation of SH signal as a function of time and $\langle SH\rangle$ is the ensemble average of the SH signal. The normalized autocorrelation, $G(\tau)$, of the measured temporal fluctuations in the SH signal, $SH(t)$, can then be written as[1]

$$G(\tau) = \frac{\langle \delta SH(t+\tau)\delta SH(t)\rangle}{\langle SH(t)\rangle^2} \quad (4)$$

where τ is the time step used to cross-correlate the signal with itself.

In FCS, the fluctuations giving rise to the measured fluorescence signal are a result of any dynamic processes of the molecules within the observation volume on the time scale of τ.[1,18] When applying FCS to the reversible binding of molecules at a surface, the dynamic processes contributing to the observed fluctuation include diffusion in and out of the observation volume and absorption and desorption of the molecules to the surface.[1,17,18] Under these conditions, the autocorrelation function, $G(\tau)$, is composed of functions related to both surface binding kinetics and diffusion of molecules in solution.[17] For SHCS, the measured fluctuations from molecules in solution are eliminated due to the surface

dx.doi.org/10.1021/ac4018742 | Anal. Chem. 2013, 85, 8429−8435

specificity of the SHG process. The autocorrelation function, $G(\tau)$, is then greatly simplified as the only contributing factor to the correlated fluctuations in the SH signal are from the surface binding kinetics of the molecule being monitored. This situation is similar to the theoretical case of FCS when there are no molecules in solution. Therefore, the FCS theory developed by Starr and Thompson for the determination of surface binding kinetics in the limit of no molecules in solution can be implemented to determine the adsorption and desorption rates of molecules associating with a surface using the time dependence of the autocorrelated SH signal.[17]

The small molecule SBN, investigated in this study, has previously been shown to reversibly bind to a lipid bilayer.[25] Because of the reversible binding of SBN to a lipid bilayer and the finite number of binding sites on the PSLB, typical bimolecular reversible binding at a surface can be assumed.[25] In this binding model an average solution concentration of molecules A are in dynamic equilibrium with unoccupied surface binding sites with an average density B, and interact to produce an average density of surface-bound complexes, C, a general mechanism can be written as

$$A + B \underset{k_{on}}{\overset{k_{off}}{\leftrightharpoons}} C \tag{5}$$

The rate constant describing the forward reaction is k_{on}, and the reverse reaction rate is described by the dissociation rate constant, k_{off}. The equilibrium binding constant, K_a, which describes the complete reaction, can then be determined using

$$K_a = \frac{k_{on}}{k_{off}} \tag{6}$$

Assuming any surface diffusion through the observation area is much faster than the adsorption and desorption rates and using a typical Langmuir bimolecular binding model, the normalized time dependent autocorrelation function, $G(\tau)$, will have the form of a first-order exponential decay given by[18]

$$G(\tau) = \frac{1}{N_C}\frac{k_{off}}{k_{on}[A]}\exp[-(k_{on}[A] + k_{off})\tau] \tag{7}$$

where N_C is a normalization constant that accounts for the surface density of adsorbed analyte, [A] is the bulk solution analyte concentration, and k_{on} and k_{off} are the adsorption and desorption rates, respectively. Using eq 7, both the adsorption and desorption rates can be retrieved from the autocorrelation of the SH signal from a single analyte concentration.

EXPERIMENTAL SECTION

Materials. 1,2-Dioleoyl-*sn*-glycero-3-phosphocholine (DOPC) from Avanti Polar Lipids and SBN from Sigma-Aldrich were both used as received. All water used in the experiments was from a Nanopure Infinity Ultrapure water system with a minimum resistivity of 18.2 MΩ cm. Phosphate buffered saline (PBS) was made from 50 mM $Na_2HPO_4{\cdot}7H_20$ and 100 mM NaCl in water and adjusted to a pH of 7.4 using NaOH. SBN was dissolved in PBS pH 7.4 to the desired working concentrations (0.43 nM to 20 μM for the isotherm studies and 55 μM for the autocorrelation studies). Custom manufactured full spectrum grade (IR/UV) fused silica prisms (Almaz Optics) were used as substrates for the planar supported lipid bilayers (PSLBs). The prisms were cleaned by immersion in a solution of 70% sulfuric acid and 30% hydrogen peroxide overnight. (CAUTION: This solution is a strong oxidant and reacts violently with organic solvents. Extreme caution must be taken when handling the solution). Prior to use, the prisms were rinsed with copious amounts of water and cleaned with Ar plasma (Harrick Scientific Plasma Cleaner/Sterilizer) for 3 min. After plasma cleaning the prism, it was then mounted in a custom built Teflon flowcell (volume of 0.4 mL).

PSLBs. All lipids were dissolved in chloroform, evaporated under a gentle stream of N_2(g), and vacuum-dried overnight to remove residual solvent. The formation of small unilamellar vesicles (SUV) solutions were performed by resuspending the dried lipids in PBS to a concentration of 1 mg/mL followed by vortexing and bath sonication for 10−20 min until the solutions were clear. A PSLB was formed on the silica prism via vesicle fusion by incubating the surface with the SUV solution for 20 min at room temperature. PBS was then flushed through the flowcell to remove any unbound lipids in solution.

SHG Measurements. The counter-propagating SHG setup used for these experiments has been described in detail previously.[26] Briefly, the second harmonic output (532 nm) of a Nd:YAG laser (Continuum, Surelite II, 20 Hz, 7 ns pulse) was directed toward a prism/water interface under total internal reflection. The laser intensity at the sample was 24 mJ/pulse and the beam size was ∼1 mm^2 in diameter. The reflected beam was steered back on itself to overlap spatially and temporally with the incident beam, resulting in an SH emission at 266 nm along the surface normal. Two notch filters (Semrock) were used to allow only light from the SHG signal through before collection by a solar-blind photomultiplier tube (Hamamatsu).

SHCS. Autocorrelation experiments of SBN association to a DOPC bilayer were performed using a concentration well above the SBN saturation concentration, 55 μM, after a steady-state response had been reached. Single shot data collection was recorded so that the time interval was dictated by the 20 Hz laser (50 ms). Each data set was collected for 100 s such that there were 2 000 data points. For one experiment, five data sets were consecutively collected totaling 10 000 data points. A total of 25 data sets from 5 separate experiments were each cross-correlated with itself and then averaged to form the autocorrelation.

Adsorption Isotherms. For the standard isotherm study of SBN adsorption to a DOPC bilayer, three independent binding experiments and three control experiments were conducted. For these experiments, increasing concentrations of SBN ranging from 0.43 nM to 20.0 μM were injected and allowed to reach equilibrium between the bulk solution and bilayer. To compensate for the bulk SBN depletion, an injection of the same SBN concentration was made every 5 to 10 min until a steady-state response was reached. Typically, the lowest concentrations required between 1 to 2 h to reach equilibrium. The SH intensity was recorded using time averaging of 100 samples per data point at 10 min intervals for 3 to 5 min to allow kinetic measurements to be made as a function of time. Isotherm measurements were made using only the SH intensity collected at steady-state equilibrium for each SBN concentration. To compare multiple data sets, a two-point normalization to a 10 mM KOH solution and a solution of PBS pH 7.4 was performed on the measured SH intensity, followed by subtraction of the background signal before addition of SBN.

RESULTS AND DISCUSSION

The SH signal collected for every pulse of the 20 Hz laser as a function of time for a bulk solution concentration of 55 μM

dx.doi.org/10.1021/ac4018742 | Anal. Chem. 2013, 85, 8429−8435

SBN intercalating into a DOPC bilayer is shown in the inset of Figure 2A. The fluctuations in the SH signal primarily arise

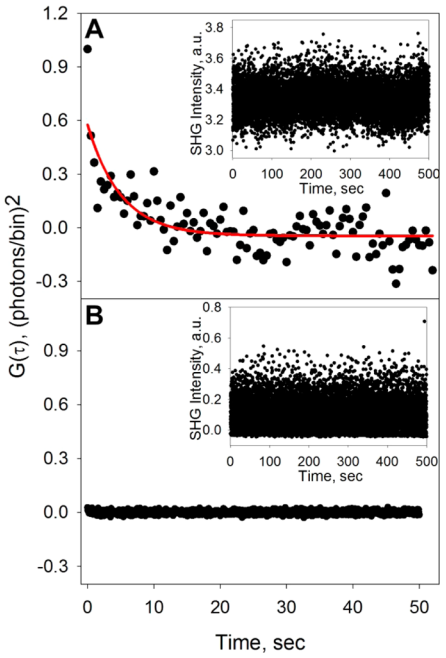

Figure 2. Autocorrelation data for (A) SBN intercalating into a DOPC bilayer with fit to eq 7 indicated by the red line and (B) a pure DOPC bilayer normalized to the autocorrelation shown in part A for comparison. Insets are representative examples of the measured fluctuations in SH signal that were used for the autocorrelation analysis.

from uncorrelated photon shot noise, but some of the fluctuations arise from correlated dynamic molecular events occurring at the surface. To extract the correlated events, the fluctuations in the SH signal were autocorrelated. The measured fluctuations from the mean SH signal were assumed to be linear as discussed above. Analysis of the square root of the SH intensity deviations (data not shown) confirms this assumption to be accurate and, in fact, produces the same autocorrelation function. The normalized autocorrelation, $G(\tau)$, from 25 data sets of SBN intercalating into a DOPC bilayer is shown in Figure 2A, where every 10th data point is shown for ease of visualization. The first point of the autocorrelation has been removed, as it contains the contributions from photon shot noise.[13] Autocorrelation was also performed on 20 data sets of a pure DOPC bilayer in order to verify there was indeed no correlation of the SH signal obtained from the bilayer alone or from photon shot noise on the time scale of the molecular dynamic events on the surface, as this would contribute to the correlation seen for the association of SBN to the DOPC bilayer. The resulting autocorrelation from the pure DOPC bilayer is shown in Figure 2B with the raw collected SH signal fluctuations shown in the inset.

The DOPC autocorrelation was normalized to the autocorrelation obtained for SBN associating to DOPC in order to compare their relative magnitudes. No correlation from the DOPC bilayer or from photon shot noise was observed. This means the observed autocorrelation in Figure 2A is solely due to the surface binding kinetics of SBN to DOPC. The autocorrelation data of SBN intercalating into a DOPC bilayer, Figure 2A, were fit to eq 7 with the parameters of N_C, k_{on}, and k_{off} and the results are given in Table 1. The

Table 1. Measured Surface Adsorption Rate (k_{on}), Desorption Rate (k_{off}), and Equilibrium Binding Constant (K_a) for SBN Intercalating into a DOPC Bilayer Obtained Using SHCS and from a Typical Binding Isotherm

	k_{on} ($\times 10^3$ s^{-1} M^{-1})	k_{off} ($\times 10^{-4}$ s^{-1})	K_a ($\times 10^6$ M^{-1})
SHCS	2.7 ± 0.1	9 ± 4	3.0 ± 1.3
isotherm	1.4 ± 0.4	6 ± 1	2.6 ± 0.2

adsorption and desorption rates from the nonlinear least-squares regression fit of eq 7 are 2.7 ± 0.1 × 10^3 s^{-1} M^{-1} and 9.0 ± 4 × 10^{-4} s^{-1}, respectively. Using eq 6, the equilibrium binding constant, K_a, is calculated to be 3.0 ± 1.3 × 10^6 M^{-1}

The large error seen in the predicted desorption rate is due to the high degree of correlation between the fitting parameters, N_C and k_{off}. In order to determine a more accurate k_{off}, desorption of SBN from a DOPC bilayer was monitored over time after flushing the flowcell with excess PBS buffer, shown in Figure 3.

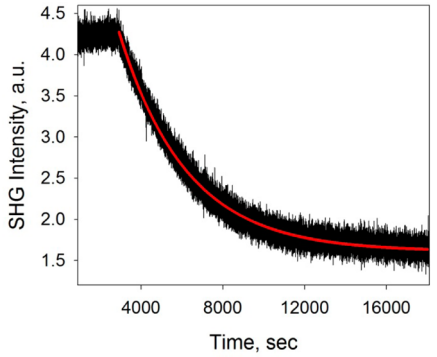

Figure 3. Desorption of SBN from a DOPC bilayer with a fit to an exponential decay indicated by the red line.

The resulting measured desorption rate is 4.0 ± 1.4 × 10^{-4} s^{-1}. The rate determined from the desorption of SBN from the DOPC bilayer is statistically the same as the rate determined using the normalized autocorrelation function in eq 7 as well as the calculated K_a of 6.8 ± 2.4 × 10^6 M^{-1}. The good agreement between the independently determined k_{off} value and that determined from SHCS demonstrates the ability of SHCS to accurately determine the adsorption and desorption rates simultaneously for molecules associating to a surface. Since these experiments were designed to show the feasibility of SHCS to determine surface binding kinetics, only one concentration well above the detection limit was used. However, a rough estimate of the sensitivity of SHCS can be made for this data using the known sensitivity of the PMT detector, the measured background signal (before SBN has been added), the incident laser power at the surface and the known maximum surface excess of SBN, 2.6 ± 0.3 × 10^{13} molecules cm^{-2} published by Conboy and Kriech.[25] The calculated limit of detection for SBN is 6.1 ± 0.7 × 10^9 molecules or 10 ± 1 fmol. This limit of detection is on the same order of magnitude as that obtained by Conboy and Kriech for SH spectroscopy.[25] It is important to remember this is only an approximation, and as mentioned before the sensitivity of SHCS has not fully been investigated. Methods to improve the

dx.doi.org/10.1021/ac4018742 | Anal. Chem. 2013, 85, 8429−8435

signal-to-noise ratio will significantly lower the limit of detection and are currently under investigation.

The surface binding kinetics obtained here using SHCS were also compared to those obtained by Kriech and Conboy.[25] Although the adsorption rate, $5.7 \pm 3.8 \times 10^3$ M^{-1}, reported by Kriech and Conboy is on the same order of magnitude as the adsorption rate obtained using SHCS, the desorption rate obtained using both SHCS and a simple desorption experiment is 2 orders of magnitude lower than the previously reported rate of $2.1 \pm 3.8 \times 10^{-2}$ s^{-1}.[25] The discrepancy in k_{off} makes the calculated K_a value obtained in the current study an order of magnitude higher than the value, $3.0 \pm 0.1 \times 10^5$ M^{-1} reported by Kriech and Conboy.[25] There are a few experimental differences, such as the type of lipid used and the incubation time for SBN to bind to the PSLB, which could explain some of the difference between the k_{off} reported here and the k_{off} reported by Kriech and Conboy. However, the primary source for the discrepancy between the desorption values is most likely related to the substantial decrease in the limit of detection (~2 orders of magnitude smaller) of the SHG instrument used here. The calculated limit of detection of our current SHG apparatus is 0.040 ± 0.005 fmol compared to 4.5 fmol reported by Kriech and Conboy.[25] The lower limit of detection seen here is a result of our notch filters having ~60% higher transmission efficiency at the SH wavelength of 266 nm and higher rejection in the visible region of the spectrum than those used by Kriech and Conboy. The lowest solution concentration of SBN that was detectable in this study was 43 nM (shown in Figure 5 inset), whereas Kriech and Conboy were only able to detect as low as 1 μM.[25] The ability to detect a lower concentration than 1 μM in the case of SBN associating to DOPC is extremely important as the resulting fit to the binding isotherm is drastically affected. The deviation from a linear response at very low bulk concentrations (<50 nM) is a result of approaching the limit of detection and not a deviation from a Langmuir isotherm as is apparent in the complete isotherm shown in Figure 5. Since 1 μM is at the very end of the linear region of the isotherm, where the adsorption and desorption rates are highly dependent on the slope, there is not enough data to adequately determine the binding kinetics. In order to obtain more accurate binding kinetics, lower concentrations within the linear region of the binding isotherm must be obtained, as is possible in these studies.

In order to have a more accurate comparison for the SBN binding kinetics obtained using SHCS, an independent binding isotherm was obtained. The data was collected as a function of time at 10 min intervals for bulk SBN concentrations ranging from 0.43 nM to 20.02 μm. To ensure that steady-state equilibrium had been reached, at each concentration multiple injections of the same concentration were made until there was no additional increase in SH signal. Although much lower concentrations (down to 43 nM) could be detected, it was unnecessary to start at such a low concentration as the concentration of 0.5 μM gave enough data in the linear region of the binding isotherm to obtain an accurate fit. The adsorption and desorption rates of SBN intercalating into a DOPC bilayer can be determined by assuming a Langmuir binding model where the SBN adsorption rate is first-order with respect to both the bulk SBN concentration, C_{bulk}, and the fraction of the unbound binding sites, $(1 - \theta)$, and the desorption rate of SBN is first order with respect to the fraction of bound SBN, θ. The rate of change in the bound SBN is then given by

$$\frac{d\theta}{dt} = k_{on}C_{bulk}(1 - \theta) - k_{off}\theta \quad (8)$$

The fraction of bound SBN, θ, is taken as the measured $(I_{SHG})^{1/2}$ divided by measured SH intensity at the saturation concentration, $(I_{SHG}^{Max})^{1/2}$. The SHG data for SBN intercalating into a DOPC bilayer in terms θ versus time for the concentration range of 0.50–20.02 μM is plotted in Figure 4.

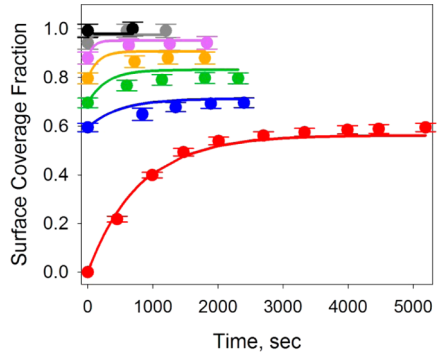

Figure 4. Fraction of surface coverage, θ, as a function of time for SBN intercalating into a DOPC bilayer measured at the following SBN bulk concentrations: 0.5 μM (red), 1.01 μM (blue), 2.01 μM (green), 4.0 μM (orange), 8.05 μM (pink), 16.06 μM (gray), and 20.02 μM (black). The solid lines represent the global fits to eq 9.

Since the SHG isotherm data was collected by consecutively increasing the bulk SBN concentration until saturation was reach in a single experiment without any desorption step in between consecutive concentrations, the initial time of each concentration was set to zero by setting the initial fraction of bound SBN equal to the calculated θ for the previous SBN concentration at saturation, as shown in Figure 4. After solving eq 8 with the boundary condition that the initial fraction of bound SBN is zero, θ_0, at time $t = 0$ and at any time $t > 0$ the fraction of bound SBN is some value θ, the adsorption and desorption rate of the data were determined by simultaneously fitting all data in Figure 4 to the following equation,

$$\theta = \frac{k_{on}C_{bulk}}{k_{on}C_{bulk} + k_{off}}[1 - \exp(-k_{on}C_{bulk} + k_{off})t] + \theta_0 \exp(-k_{on}C_{bulk} + k_{off})t \quad (9)$$

The adsorption and desorption rates obtained from the nonlinear least-squares regression fit to eq 9 are $1.4 \pm 1.4 \times 10^3$ s^{-1} M^{-1} and $5.6 \pm 1 \times 10^{-4}$ s^{-1}, respectively, giving a K_a of $2.6 \pm 0.2 \times 10^6$ M^{-1} (shown in Table 1). The values for k_{on}, k_{off}, and K_a obtained using the kinetic isotherm data are in good agreement with those obtained using SHCS.

Next, a thermodynamic equilibrium binding isotherm was obtained by taking only the SH intensity value for each concentration at steady-state equilibrium (the last data point for each concentration in Figure 4). The thermodynamic binding isotherm obtained for SBN intercalating into a DOPC bilayer is shown in Figure 5. The SH intensity increases with increasing concentration of SBN until it reaches saturation concentration in the membrane. The SH intensity is normalized and the errors are from 3 separate experiments. Assuming a Langmuir binding model, the SH signal will take on the form of the following expression:

dx.doi.org/10.1021/ac4018742 | Anal. Chem. 2013, 85, 8429–8435

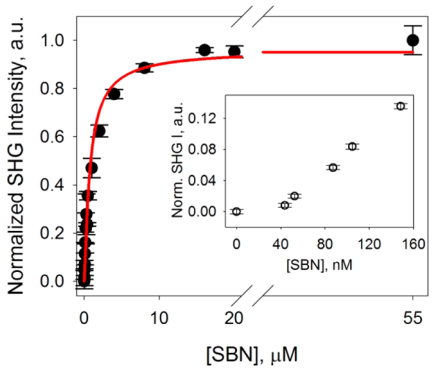

Figure 5. SH intensity of SBN intercalated into a DOPC bilayer versus bulk SBN concentration. The red line is the fit to the Langmuir model (eq 10), and the error bars represent the standard deviation from the SHG measurement. Inset is an enlargement of the bulk SBN concentrations in the nanomolar region.

$$I_{SHG} \propto \left(\frac{\sqrt{I_{SHG}^{max}} K_a [C_{bulk}]}{1 + K_a [C_{bulk}]} \right)^2 \quad (10)$$

The complete derivation of this expression has been derived in a previous publication from our group.[27] The equilibrium binding constant, K_a, determined from the fit to eq 10 is $2.4 \pm 0.2 \times 10^6$ M^{-1}. This value is in good agreement with the K_a obtained using SHCS.

The good agreement between the results obtained from SHCS and those measured via a classic adsorption isotherm demonstrates the validity of using SHCS to determine the binding kinetics of molecules at a surface. Additionally, the time required to collect the SHCS data was much shorter than the time required to collect the binding isotherm data. For example, the autocorrelation data collection took less than 2 h, whereas the binding isotherm of SBN took 6 h to complete. Moreover, multiple injections of SBN were not necessary over the course of collection of the SHCS data as compared to the isotherm data where an injection was made every 10 min to compensate for bulk SBN depletion and to allow kinetic information to be determined. Another advantage of SHCS is the simultaneous determination of both the adsorption and desorption rates using only a single concentration of analyte. It is true that determining the desorption rate in a separate experiment provides a statistically better fit to the autocorrelation function; however, since the desorption rate determined separately was within error of the desorption rate from SHCS, it is still possible to determine both the adsorption and desorption rate using a single analyte concentration with SHCS. Alternatively, if additional SBN concentrations were also examined using SHCS, a global fit to all concentrations would provide a statistically better fit to the autocorrelation function and more accurate kinetic information could be obtained without requiring the desorption rate to be determined separately. In addition to the advantages over conventional isotherm studies, SHCS also offers several advantages over the more commonly used FCS method. The most obvious advantage is that no exogenous label is required to obtain the data. This eliminates many obstacles seen with FCS, such as problems associated with photobleaching and the unavoidable contribution from solution phase species to the observed fluctuations. In addition, the ability of SHCS to only detect the molecules bound to the surface simplifies the autocorrelation function used to retrieve the binding kinetics as compared to FCS because diffusion of molecules in solution can be neglected, which leaves only the surface binding kinetics of molecules contributing to the fluctuations seen in the SH signal. These advantages make SHCS an attractive and efficient method to directly determine the binding kinetics of molecules at a surface.

SUMMARY

In these studies, the binding kinetics of SBN intercalating into a DOPC planar supported lipid bilayer was investigated using both a traditional binding isotherm and SHCS. The adsorption and desorption rates as well as the equilibrium binding constant, determined using both methods, were statistically identical within the 99% confidence interval. These results demonstrate the validity of using the surface specific and label-free method of SHCS to examine molecular interactions at a surface. Although the desorption rate was obtained *a priori* in order to decouple the autocorrelation fitting parameters and reduce the error in the resulting values, it is not wholly necessary. The lower total analyte quantity required and the reduced time to obtain the surface binding kinetics makes SHCS an attractive analytical tool for many bioanalytical systems where analyte and time are often scarce. Moreover, the surface specificity and label-free nature of SHCS eliminate some of the challenges seen in FCS due to fluorophores and diffusion of molecules in bulk solution. Since the only contribution to the fluctuations in SH is from surface associated molecules, SHCS data analysis is greatly simplified. The simplicity and efficiency of SHCS makes it a new and valuable technique to directly and precisely ascertain the binding kinetics of molecules at a surface without a label.

AUTHOR INFORMATION

Corresponding Author

*E-mail: conboy@chem.utah.edu.

Notes

The authors declare no competing financial interest.

ACKNOWLEDGMENTS

The authors acknowledge the financial support from the National Institutes of Health (Grant R01-GM068120). Any opinions, findings, conclusions, or recommendations expressed in this material are those of the authors and do not necessarily reflect the views of the National Institutes of Health.

REFERENCES

(1) *Topics in Fluorescence Spectroscopy*; Lakowicz, J. R., Ed.; Plenum Press: New York, 1991; Vol. *1*.
(2) Magde, D.; Elson, E.; Webb, W. W. *Phys. Rev. Lett.* **1972**, *29*, 705.
(3) Koppel, D. E.; Axelrod, D.; Schlessinger, J.; Elson, E. L.; Webb, W. W. *Biophys. J.* **1976**, *16*, 1315.
(4) Magde, D.; Elson, E. L.; Webb, W. W. *Biopolymers* **1974**, *13*, 29.
(5) Fahey, P. F.; Koppel, D. E.; Barak, L. S.; Wolf, D. E.; Elson, E. L.; Webb, W. W. *Science* **1977**, *195*, 305.
(6) Andries, C.; Guedens, W.; Clauwaert, J.; Geerts, H. *Biophys. J.* **1983**, *43*, 345.
(7) Palmer, A. G., III; Thompson, N. L. *Proc. Natl. Acad. Sci. U.S.A.* **1989**, *86*, 6148.
(8) Petersen, N. O.; Johnson, D. C.; Schlesinger, M. J. *Biophys. J.* **1986**, *49*, 817.
(9) Borejdo, J. *Biopolymers* **1979**, *18*, 2807.
(10) Lieto, A. M.; Cush, R. C.; Thompson, N. L. *Biophys. J.* **2003**, *85*, 3294.
(11) Thompson, N. L.; Axelrod, D. *Biophys. J.* **1983**, *43*, 103.

(12) Hansen, R. L.; Harris, J. M. *Anal. Chem.* **1998**, *70*, 4247.
(13) Hansen, R. L.; Harris, J. M. *Anal. Chem.* **1998**, *70*, 2565.
(14) Bismuto, E.; Gratton, E.; Lamb, D. C. *Biophys. J.* **2001**, *81*, 3510.
(15) McCain, K. S.; Schluesche, P.; Harris, J. M. *Anal. Chem.* **2004**, *76*, 930.
(16) Ruckstuhl, T.; Krieg, A. *Anal. Chem.* **2005**, *77*, 2656.
(17) Thompson, N. L.; Navaratnarajah, P.; Wang, X. *J. Phys. Chem. B* **2011**, *115*, 120.
(18) Starr, T. E.; Thompson, N. L. *Biophys. J.* **2001**, *80*, 1575.
(19) Thompson, N. L.; Burghardt, T. P.; Axelrod, D. *Biophys. J.* **1981**, *33*, 435.
(20) Maiti, S.; Haupts, U.; Webb, W. W. *Proc. Natl. Acad. Sci. U.S.A.* **1997**, *94*, 11753.
(21) Yan, E. C. Y.; Eisenthal, K. B. *J. Phys. Chem. B* **2000**, *104*, 6686.
(22) Shen, Y. R. *The Principles of Nonlinear Optics*; Wiley: New York, 1984.
(23) Nguyen, T. T.; Conboy, J. C. *Anal. Chem.* **2011**, *83*, 5979.
(24) Kubo, R.; Matsuo, K.; Kitahara, K. *J. Stat. Phys.* **1973**, *9*, 51.
(25) Kriech, M. A.; Conboy, J. C. *Appl. Spectrosc.* **2005**, *59*, 746.
(26) Kriech, M. A.; Conboy, J. C. *J. Opt. Soc. Am. B: Opt. Phys.* **2004**, *21*, 1013.
(27) Nguyen, T. T.; Sly, K. L.; Conboy, J. C. *Anal. Chem.* **2012**, *84*, 201.

dx.doi.org/10.1021/ac4018742 | *Anal. Chem.* 2013, 85, 8429−8435